

**Controlled delivery of SDF-1 α and IGF-1: CXCR4+ cell recruitment and functional skeletal muscle recovery**

Journal:	<i>Biomaterials Science</i>
Manuscript ID:	BM-ART-07-2015-000233
Article Type:	Paper
Date Submitted by the Author:	07-Jul-2015
Complete List of Authors:	Rybalko, Viktoriya; University of Texas@austin, Pham, Chantal; University of Texas@austin, Hsieh, Pei-Ling; University of Texas@austin, Hammers, David; University of Texas@Austin, Kinesiology Merscahm-Banda, Melissa; University of Texas@Austin, Kinesiology Suggs, Laura; Univ Texas Austin, Farrar, Roger; Univ of Texas @austin, Kinesiology

22 **ABSTRACT**

23 Therapeutic delivery of regeneration-promoting biological factors directly to the site of injury
24 has demonstrated its efficacy in various injury models. Several reports describe improved tissue
25 regeneration following local injection of tissue specific growth factors, cytokines and
26 chemokines. Evidence exists that combined cytokine/growth factor treatment is superior for
27 optimizing tissue repair by targeting different aspects of the regeneration response. The purpose
28 of this study was to evaluate the therapeutic potential of the controlled delivery of stromal cell-
29 derived factor-1alpha (SDF-1 α) alone or in combination with insulin-like growth factor-I (SDF-
30 1 α /IGF-I) for the treatment of tourniquet-induced ischemia/reperfusion injury (TK-I/R) of
31 skeletal muscle. We hypothesized that SDF-1 α will promote sustained stem cell recruitment to
32 the site of muscle injury, while IGF-I will induce progenitor cell differentiation to effectively
33 restore muscle contractile function after TK-I/R injury while concurrently reducing apoptosis.
34 Utilizing a novel poly-ethylene glycol PEGylated fibrin gel matrix (PEG-Fib), we incorporated
35 SDF-1 α alone (PEG-Fib/SDF-1 α) or in combination with IGF-I (PEG-Fib/SDF-1 α /IGF-I) for
36 controlled release at the site of acute muscle injury. Despite enhanced cell recruitment and
37 revascularization of the regenerating muscle after SDF-1 α treatment, functional analysis showed
38 no benefit from PEG-Fib/SDF-1 α therapy, while dual delivery of PEG-Fib/SDF-1 α /IGF-I
39 resulted in IGF-I-mediated improvement of maximal force recovery and SDF-1 α -driven *in vivo*
40 neovasculogenesis. Histological data supported functional data, as well as highlighted the
41 important differences in the regeneration process among treatment groups. This study provides
42 evidence that while revascularization may be necessary for maximizing muscle force recovery,
43 without modulation of other effects of inflammation it is insufficient.

44

45

46 **INTRODUCTION**

47 Skeletal muscle tissue has a remarkable ability to regenerate. Nevertheless, muscle regenerative
48 capacity is reduced during ageing and can be greatly compromised following severe injuries [1].
49 Functional deficits are commonly a consequence of impaired regenerative responses, leading to
50 partial or complete loss of muscle function [2].

51 In animal models cell-based therapies have been used successfully to enhance muscle
52 regeneration [3] [4-9]. Transfers of myoblasts/satellite cells [10], mesenchymal cells [11], bone
53 marrow-derived stem cells [12, 13], peripheral blood-derived stem cells [14] and other tissue
54 resident stem cell populations [3, 8] with multi-lineage potential are tested with hopes to develop
55 viable treatments for skeletal muscle injuries and muscle wasting disorders. In pre-clinical trials
56 myoblast transplantation showed great promise for the treatment of localized muscular
57 dystrophies as well as several conditions such as urinary and anal incontinence [7]. Several
58 serious challenges still preclude the widespread use of stem-cell based therapies in clinic: 1) the
59 need for standardized *in vitro* culture systems to raise sufficient and homogeneous stem cell
60 populations [6, 15]; and 2) the ability to control cell fate before and after transplantation to avoid
61 undesirable transdifferentiation and potential for malignant transformation [16]. Although, such
62 issues as immune rejection, poor survival, limited trafficking and engraftment at the site of injury
63 are existing limitations [7], several studies still show transient benefits from stem cell therapies
64 due to the modulation of local inflammation through the release of anti-inflammatory mediators,
65 as well as secondary effects on resident or locally recruited cells [12, 13, 17-21]. Overall, with
66 better characterization of microenvironmental components influencing the outcome of tissue

67 regeneration, more combination therapies are likely to emerge including simultaneous delivery
68 of several growth factors, cytokines and chemokines, co-transplantation of multiple cell
69 populations and combinatorial treatments with both growth factors/cytokines/chemokines and
70 cells. As such, co-transplantation studies using innate immune cells and human myoblasts were
71 effective at stimulating myoblast proliferation and engraftment into mouse dystrophic muscle
72 [22]. Co-delivery of SDF-1 α transgene and endothelial progenitors enhanced cell engraftment
73 and subsequent angiogenesis of the ischemic muscle [23]. Despite recent developments, the use
74 of stem cell therapies is precluded by safety concerns. Therefore, identification of stem cell-
75 trophic and regulatory factors and their subsequent incorporation into biodegradable matrices for
76 the delivery into injured tissues represents a safer alternative to cell-based therapies.

77 Various synthetic scaffolds have been designed to deliver biomolecules to the site of acute injury
78 [24-26]. Polyethylene glycol (PEG) is a synthetic polymer. It has been used extensively for
79 delivering covalently attached proteins *in vivo*. PEG-fibrinogen (PEG-Fib) results from coupling
80 of PEG with fibrinogen molecules, enabling generation of a biodegradable PEG-Fib matrix after
81 thrombin addition, while maintaining the capacity to covalently bind various protein factors. This
82 biological scaffold is useful in several aspects: 1) It provides controlled release of conjugated
83 protein factors; 2) It decreases the rate of protein clearance by the immune system; and 3) It
84 localizes the delivery of protein factors to a particular site or tissue [27]. Recently our group used
85 PEG-Fib to conjugate and deliver IGF-I to improve functional recovery of skeletal muscle
86 following TK-I/R injury [28]. Zhang et al. [29] successfully used PEG-Fib matrix-based
87 delivery of SDF-1 α to enhance myocardial remodeling. Delivery of SDF-1 α as well as other
88 cytokines, chemokines and growth factors directly to the site of acute injury has been
89 successfully accomplished by other research groups [24-26].

90 SDF-1 α or CXCL12 is a small pro-inflammatory cytokine. Its expression is transiently induced
91 after ischemic injury in several tissues including skeletal muscle [30, 31]. During inflammation
92 and injury, SDF-1 α was shown to be the most potent chemoattractive signal for CXCR4⁺ cells
93 and is considered a major stem cell homing factor [32, 33]. CXCR4-expressing cells include
94 hematopoietic stem cells [29], endothelial progenitor cells [23, 32, 34], mesenchymal stem cells
95 [35], satellite cells [36] as well as monocytes and lymphocytes[33]. In the models of ischemic
96 limb damage, SDF-1 α was shown to restore perfusion and enhance regeneration via recruitment
97 of a CXCR4⁺ cell fraction with pro-angiogenic properties [25, 37]. In contrast, in a model of
98 kidney I/R injury SDF-1 α was shown to have no effects on recruitment of stem cells to the
99 kidney, however, disruption of SDF- α 1 severely increased renal dysfunction and injury [38, 39]
100 highlighting its requirement in locally mediated tissue repair. Injury models of myocardial
101 regeneration provide substantial evidence that SDF-1 α mediated therapies are beneficial due to
102 improved survival of local and recruited progenitor cells as well as enhanced neovascularization
103 [29, 40]. Overall, strong evidence exists for the requirement of SDF-1 α -mediated signaling in
104 orchestration of tissue regeneration, albeit the exact mechanisms of action may be tissue- and
105 injury- specific.

106 IGF-I is a pro-regenerative [41], anti-inflammatory growth factor [42]. Major effects of IGF-I
107 include regulation of myoblast proliferation, differentiation and survival [41, 43], modulation of
108 inflammatory response [42], stimulation of anabolic pathways [44-46] and atrophy prevention
109 [47]. Our group has previously shown major pro-regenerative effects of IGF-I following *in vivo*
110 PEG-Fib/IGF-I delivery into the TK-I/R injured muscle [28].

111 Motivated by our previous findings that PEG-Fib/IGF-I delivery significantly enhances muscle
112 regeneration we wanted to address the therapeutic efficacy of combined PEG-Fib/SDF-1 α /IGF-I

113 and PEG-Fib/SDF-1 α therapies on functional muscle regeneration following TK-I/R injury. We
114 hypothesized that elevating and maintaining SDF-1 α levels via PEG-Fib-mediated release at the
115 site of I/R injury will promote the recruitment of resident, as well as circulating CXCR4-
116 expressing progenitor cells, to the site of injury. In turn, combined incorporation of IGF-I into a
117 biodegradable matrix should further stimulate stem cell proliferation and differentiation to
118 subsequently improve functional regeneration of TK-I/R injured muscle.

119 **MATERIALS AND METHODS**

120 *Animals*

121 Male Sprague–Dawley rats (6–9 months; Charles River) were maintained on a 12-hour light/dark
122 cycle and housed individually. Animals were allowed ad libitum access to food and water. All
123 experimental procedures were approved and conducted in accordance with guidelines set by the
124 University of Texas at Austin and the Institutional Animal Care and Use Committee.

125 *Tourniquet Application*

126 The 2-hour tourniquet-induced ischemia/reperfusion (TK-I/R) model of skeletal muscle injury
127 was induced as previously described [2]. Briefly, randomly selected hind limb was elevated and
128 a pneumatic tourniquet cuff (D.E. Hokanson, Inc.; Bellevue, WA) was placed proximal to the
129 knee. The cuff was inflated to 250 mm Hg using the Portable Tourniquet System (Delfi Medical
130 Innovations Inc.; Vancouver, BC, Canada) for 2 hours. During the course of this procedure, rats
131 were anesthetized with 2% to 2.5% isoflurane and body heat was maintained with the use of a
132 heat lamp. The analgesic, carprofen, was administered prior to tourniquet application, 12- and
133 24- hours post-TK-I/R injury for pain management.

134

135

136 ***PEGylated Fibrin Preparation and Delivery***

137 Protein factor conjugated PEGylated fibrin gel was prepared as previously described [27, 29].
138 Briefly, human fibrinogen (Sigma-Aldrich Co.; St. Louis, MO) was reconstituted in Tris-
139 buffered saline (40 mg/mL, pH 7.8) and reacted with bifunctional SG-PEG-SG (NOF America
140 Corp, Irvine, CA) in 5:1 PEG:fibrinogen molar ratio with or without the addition of rat SDF-1 α
141 (PeproTech Inc.; Rocky Hill, NJ) and human IGF-I (Pepro Tech Inc.; Rocky Hill, NJ). Gel
142 polymerization was induced by the addition of 25 U/mL of human thrombin (Sigma). The final
143 concentration of fibrinogen was 10 mg/mL, PEG 0.5 mg/ml, SDF-1 α 10 μ g/mL, IGF-I 25 μ g/ml.
144 Twenty-four hours post TK-I/R injury, 0.25mL of empty PEGylated fibrin gel (Peg-Fib; n=6),
145 SDF-1 α conjugated PEGylated fibrin gel (Peg-Fib/SDF-1 α ; n=6), SDF-1 α and IGF-I conjugated
146 PEGylated fibrin gel (Peg-Fib/SDF-1 α /IGF-1; n=6) was injected into the lateral gastrocnemius
147 (LGAS) muscle of the TK-injured limb. PEG-Fib-containing treatments were injected in liquid
148 form and polymerized *in situ*. Functional assessments were performed at 14 days of reperfusion.

149 ***Functional Assessment***

150 Following 14 days of TK- I/R injury, *in situ* evaluations of lateral gastrocnemius (LGAS) force
151 production were performed on the tourniquet and contralateral leg (uninjured) as previously
152 described [2]. Briefly, animals were anesthetized with isoflurane, and the skin of the hindlimb
153 was removed to expose the hamstring. LGAS muscle was isolated; innervation to the medial
154 GAS was removed. The Achilles tendon was attached to the lever arm of a dual mode
155 servomotor (Aurora Scientific Model 310B Inc.; Aurora, ON, Canada). The muscle was
156 stimulated using a stimulator (A-M Systems, Carlsborg, WA, Model 2100) with electrodes
157 applied to the tibial nerve. Optimal length (L_0) was determined by finding the length producing
158 the maximal twitch force at 0.5 Hz at 5V. Maximal peak tetanic tension (P_0) was measured at

159 150 Hz and the minimal voltage required to elicit a maximal P_o response. Each tetanic
160 contraction was followed by 2 minutes of rest. Muscle temperature was maintained with a heat
161 lamp and warm mineral oil. Data was collected and analyzed using LabView software. After the
162 completion of the contractile measurements, the muscles were harvested, weighed, embedded in
163 OCT compound, and frozen in liquid nitrogen-cooled isopentane. The muscles were stored in a -
164 80°C freezer until histological analysis.

165 *Histological Analysis, Immunofluorescent and Immunohistochemical Tissue Staining*

166 Frozen, OCT-embedded muscle samples following 14 days of recovery after I/R injury were
167 sectioned on a cryostat (Leica CM1900; Leica Microsystems Inc.; Buffalo Grove, IL) and placed
168 on a warm slide. Hematoxylin & eosin (H&E) s and Masson's trichrome (Polyscience,
169 Warrington, PA, USA) staining were performed as previously described²⁸, and slides were
170 observed with a light microscope (Nikon Diaphot, Nikon Corp.; Tokyo, Japan) with the 20X
171 objective lens. Images were taken using a mounted digital camera (Optronix Microfire;
172 Optronix; Goleta, CA). Myofiber cross-sectional area (CSA) was measured using ImageJ
173 software. Immunofluorescence protocols were previously described [48]. Briefly, sectioned
174 tissue was blocked with 5% normal donkey serum and 1% BSA in PBS, and stained with
175 primary anti-CXCR4 antibody (1:200; Novus Biologicals, Littleton, CO, USA, H00007852-
176 M04). Primary antibody staining was detected with the donkey anti-mouse IgG-TRITC
177 fluorescein (1:100; Santa Cruz Biotechnology, Inc.; Santa Cruz, CA) and counterstained with
178 DAPI (1:1000; Molecular Probe, OR, USA, D1306). CXCR4⁺ cells were identified using Leica
179 (DM IL) fluorescence microscope with the 20 × objective lens, photographed using AxioCam
180 MRm Microscope Camera and quantified using ImageJ Software. PEG-Fib group n=6; PEG-
181 Fib/SDF-1 group n=5 control leg, n=6 TK leg; PEG-Fib/SDF-1/IGF-I group n=5.

182 To measure CD31⁺ cell density, sections were stained sections with the anti-rat CD31 (PECAM-
183 1) antibody (1:25; BD Pharmingen, San Jose, CA, USA, 550300) followed by incubation with
184 the avidin-biotin enzyme kit (Vectastain ABC Kit; Vector Laboratories, Irvine, CA, USA) and
185 Pierce DAB substrate kit (Thermo Scientific, Rockford, IL, USA). CD31⁺ cell density was
186 determined from the number of CD31+ cell per muscle fiber using Image J software.

187 *Western Blotting*

188 Western blotting was performed as previously described [49]. Briefly, samples were prepared
189 and boiled in 2X Laemmli's sample buffer at a ratio of 1:1 for 5 minutes, samples were loaded
190 into each well of a 5% stacking/ 12.5% separating polyacrylamide gel. Following SDS-PAGE,
191 proteins were transferred to a PVDF membrane (Millipore) and blocked with 5% milk in 0.1%
192 Tween-20 in TBS (TBST) for 1 h. Membrane was incubated in a 1:1000 dilution of primary
193 antibody to rabbit anti-rat SDF-1 α (Peprotech) in 5% milk-TBST overnight at 4°C. Protein bands
194 were detected using 1:1000 dilution of goat anti-rabbit horseradish peroxidase-conjugated
195 secondary antibody (Pierce) in 5% milk-TBST for 2 h. Following detection of SDF-1 α protein,
196 membrane was washed, incubated in stripping buffer at 50 °C for 50 min, blocked and re-blotted
197 with primary rabbit anti-human IGF-I antibody (Peprotech) at 1:1000 dilution overnight at 4°C.
198 Secondary detection was performed as described above. Blots were imaged with the Chemidoc
199 XRS system (Bio-Rad).

200 *Statistical Analysis*

201 Functional values were analyzed using one-way ANOVA to compare groups, and the Tukey
202 post-hoc test was used to compare between data sets ($p < 0.05$). The values are represented as the
203 mean \pm SEM, unless noted otherwise.

204

205 RESULTS

206 *Identification of SDF-1 α and IGF-I by Western Blot*

207 Our group has previously shown the successful conjugation of IGF-I growth factor to PEG-Fib
208 matrix [28]. In turn, the success of SDF-1 α conjugation to PEG-Fib matrix was extensively
209 characterized by Zhang et al [29]. We utilized already established protocols to conjugate SDF-1 α
210 and IGF-I to the PEGylated fibrin matrix. By using Western Blot we confirmed the presence of
211 SDF-1 α and IGF-I in our gels (**Fig. 1**). Co-incubation of SDF-1 α and IGF-I recombinant proteins
212 with PEG-Fib matrix resulted in the formation of large PEG-Fib/SDF-1 α /IGF-I complexes
213 detected by SDF-1 α and IGF-I specific antibodies (**Fig. 1; Lane 4**). Fibrinogen (α -chain 63.5
214 kDa, β -chain 56 kDa, γ -chain 47 kDa) binds PEG (3.4 kDa), SDF-1 α (10kDa) and IGF-I
215 (7.5kDa) to form SDF-1 α /IGF-I-containing aggregates visualized at ≥ 60 kDa size. No staining
216 was detected with fibrinogen only (**Lane 2**) and PEGylated fibrinogen (**Lane 3**). Success of the
217 PEGylation procedure is reflected in the virtual absence of staining to unconjugated SDF-1 α and
218 IGF-I (**Fig. 1; Lane 4**). Our prior work has demonstrated progressive release of SDF-1 α and
219 IGF-I from PEG-Fib matrix *in vitro* [28, 29].

220 *SDF-1 α delivery promotes the persistence of CXCR4⁺ cells at the site of injury 14 days post-* 221 *reperfusion*

222 The aim of this experiment was to address whether PEG-Fib/SDF-1 α delivery was effective in
223 promoting the recruitment CXCR4⁺ cells to the site of injury. *In vitro* release kinetics showed
224 that SDF-1 α can be progressively released across 7 days [29]. We hypothesized that progressive
225 release of high concentrations of SDF-1 α from PEG-Fib matrix in the presence of the
226 inflammatory response will efficiently recruit high numbers of CXCR4⁺ cells to the site of I/R
227 injury. To address this, we used fluorescence microscopy to identify CXCR4-expressing cells

228 within TK-I/R injured skeletal muscle treated with PEG-Fib, PEG-Fib/SDF-1 α , PEG-Fib/IGF-I
229 and PEG-Fib/SDF-1 α /IGF-I at a late time point of 14 days post-reperfusion. As expected, we saw
230 significantly higher CXCR4⁺ cells present within injured muscles treated with PEG-Fib/SDF-1 α
231 (19.12 \pm 6.39% vs. 4.64 \pm 1.52%) compared to other groups (**Fig. 2**). Interestingly, the presence of
232 IGF-I was enough to suppress the effects of SDF-1 α on the recruitment of CXCR4⁺ cells (**Fig.**
233 **2**).

234 *SDF-1 α treatment of injured skeletal muscle enhances tissue revascularization*

235 CXCR4 receptor is highly expressed on endothelial cells as well as endothelial cell progenitors
236 rendering these cells sensitive to chemotactic gradients of SDF-1 α [50-52]. *In vitro* and *in vivo*
237 models show strong effects from the SDF-1/CXCR-4 axis on tissue neoangiogenesis and
238 neovascularization [50]. We addressed whether PEG-Fib/SDF-1 α treatment alone or in
239 combination with IGF-I had an effect on muscle revascularization after I/R injury. Both
240 treatment groups showed significantly higher number of CD31⁺ cells per muscle fiber (CD31⁺
241 cells/Fiber) when compared to uninjured control, PEG-Fib and PEG-Fib/IGF-I groups (**Fig.3**).
242 These findings support literature reported pro-angiogenic effects of SDF-1 α as well as provide
243 additional evidence for significant increases in revascularization of injured skeletal muscle tissue
244 after PEG-Fib-mediated SDF-1 α delivery.

245 *Improved functional regeneration after PEGylated fibrin delivery of IGF-I without* 246 *therapeutically beneficial effects from SDF-1 α*

247 We aimed to determine the efficacy of PEG-Fib-mediated controlled release of SDF-1 α and IGF-I
248 directly at the site of I/R injury on functional recovery of skeletal muscle. To address this, we
249 administered either empty PEG-Fib matrix, PEG-Fib matrix conjugated to SDF-1 α or PEG-Fib

250 matrix conjugated to SDF-1 α / IGF-I i.m. into TK-I/R injured LGAS 24 h after TK release.
251 Surprisingly, we observed no significant difference in maximum force production recovery with
252 PEG-Fib/SDF-1 α ($52.05 \pm 6.00\%$) compared to the PEG-Fib ($49.48 \pm 9.87\%$) treatment groups.
253 As expected, PEG-Fib/SDF-1 α /IGF-1 treatment resulted in improved recovery of force,
254 compared to PEG-Fib treatment ($66.50 \pm 13.37\%$ vs. $49.48 \pm 9.87\%$; $P < 0.05$) as seen in **Fig. 4**.
255 The tetanic force production in PEG-Fib/SDF-1 α /IGF-I group was similar to maximum force
256 production achieved following PEG-Fib/IGF-I treatment [28] suggesting that positive effect from
257 treatment was primarily due to the presence and bioactivity of IGF-I.
258 Specific tension values (SP_0) were determined across groups in order to normalize tetanic forces
259 to muscle cross sectional areas. Consistent with force recovery values, there were no significant
260 differences between specific tensions for the PEG-Fib ($10.59 \pm 2.41 \text{ N/cm}^2$) and PEG-Fib/SDF-
261 1 α ($10.13 \pm 2.21 \text{ N/cm}^2$) groups. There was a significant increase in specific tension in PEG-
262 Fib/SDF-1 α /IGF-1 group ($14.22 \pm 1.79 \text{ N/cm}^2$) compared to PEG-Fib and PEG-Fib/SDF-1 α
263 groups ($p < 0.05$) (**Fig. 5**). Previous delivery PEG-Fib and PEG-Fib/IGF-I into TK-I/R injured
264 muscle generated SP_0 values of $11.7 \pm 1.0 \text{ N/cm}^2$ and $14.8 \pm 0.6 \text{ N/cm}^2$ respectively [28]
265 supporting consistency of our data and highlighting the lack of SDF-1 α effect in the PEG-
266 Fib/SDF-1 α /IGF-1 group. Muscle weights across groups were not significantly different (data
267 not shown).
268 These results suggest that SDF-1 α delivery to TK-I/R injured muscle does not provide significant
269 therapeutic benefit. The beneficial effect from dual PEG-Fib/SDF1 α /IGF-I factor delivery is
270 mediated primarily by IGF-I.

271 *Histological evaluation of regenerating muscle tissue supports functional results, but points to*
272 *differences in regeneration mechanisms among groups*

273 Histological evaluation of H&E stained muscle sections at 14 days post-reperfusion in general
274 supports the functional data results described above, albeit, several important and interesting
275 distinctions are apparent between groups. For example, the PEG-Fib/SDF-1 α treatment group
276 showed a much greater distribution of smaller myofibers than the PEG-Fib group despite similar
277 contractile deficiencies (**Fig. 6A-B**). This may point to potential differences in the regeneration
278 process that may have taken place subsequent to SDF-1 α delivery. The presence of large
279 myofibers of round morphology in PEG-Fib samples is most likely an indication of an ongoing
280 regeneration process. Also, inflammatory exudate and fibrotic areas are evident during gross
281 examination of muscle sections treated with PEG-Fib (**Fig. 6A**). Persistent inflammation within
282 regenerating tissue has been associated with increased collagen deposition [53]. In turn,
283 increased fibrosis may lead to contractile dysfunction by decreasing myofiber occupancy. We
284 evaluated collagen deposition in our tissues using Trichrome staining. As expected, we saw
285 significantly higher fibrosis in PEG-Fib and PEG-Fib/SDF-1 α treated muscles (**Fig. 7**).

286 Muscles treated with PEG-Fib/SDF-1 α /IGF-I, as expected, showed almost no signs of injury
287 induced pathology and minimal fibrosis, their myofiber size distribution was comparable to that
288 of control muscle (**Fig. 6C and Fig. 7**). Histologically (H&E), muscles treated with PEG-
289 Fib/SDF-1 α /IGF-I look identical to muscle treated with PEG-Fib/IGF-I [28]. Therefore,
290 histological examination supports functional studies and provides further evidence that SDF-1 α
291 delivery via PEG-Fib does not enhance myofiber regeneration despite enhanced
292 revascularization at 14 days after I/R injury. We believe that the beneficial effect from dual PEG-
293 Fib/SDF-1 α /IGF-I delivery is mainly due to the effect of IGF-I on muscle force recovery.
294 Whether the lack of beneficial effects at 14 days in PEG-Fib/SDF-1 α group indicates delayed
295 resolution of inflammation during the acute stages of muscle regeneration was not determined.

296 In conclusion, we have shown that PEG-Fib mediated delivery of the chemokine, SDF-1 α
297 recruits CXCR4⁺ cells to the injured muscle, enhances muscle neovascularization, however, does
298 not accelerate force recovery and myofiber regeneration in I/R injured skeletal muscle at 14
299 days. In contrast, dual PEG-Fib-mediated delivery of SDF-1 α /IGF-I improves tissue
300 revascularization, leads to increased myofiber size and decreased muscle tissue fibrosis. Most
301 importantly, dual SDF-1 α /IGF-I treatment enhances functional regeneration of skeletal muscle
302 tissue after TK-I/R injury, although, positive effects on skeletal muscle force recovery appear to
303 be primarily IGF-I- mediated.

304 **DISCUSSION**

305 In this study we used a PEGylated fibrin-based matrix to deliver SDF-1 α chemokine alone or in
306 combination with IGF-I growth factor to the site of acute skeletal muscle TK-I/R injury.
307 Motivated by our previous success in the delivery of PEG-Fib/IGF-I to enhance functional
308 muscle regeneration after I/R injury [28] we aimed to address the efficiency of a combined
309 matrix-based SDF-1 α /IGF-I therapeutic approach on restoring muscle function post TK-I/R
310 injury. We found no added benefit on the restoration of muscle contractile function from
311 combined PEG-Fib/SDF-1 α /IGF-I therapy compared to PEG-Fib/IGF-I treatment at the 14 day
312 time point. However, the presence of SDF-1 α significantly enhanced muscle tissue
313 revascularization after TK-I/R injury.

314 Taking into consideration multiple literature-reported beneficial effects of SDF-1 α treatment on
315 regeneration of ischemic tissues, including skeletal muscle [25], we were surprised to find no
316 functional improvements following PEG-Fib/SDF-1 α therapy. Albeit to our knowledge, we are
317 the first group to evaluate the effect of SDF-1 α treatment on functional regeneration of skeletal

318 muscle after TK-I/R injury. In addition to functional results, histological data strengthened our
319 conclusions and provided additional evidence of ongoing degenerative/regenerative cycling at
320 the two-week time point after TK-I/R injury in the PEG-Fib/SDF-1 α treatment group
321 characterized by an abundance of smaller myofibers and increased fibrosis, despite persistence of
322 CXCR4⁺ cells at the site of injury and enhanced tissue revascularization. Although not
323 demonstrating a positive effect at this time point, our results were not completely unexpected.

324 SDF-1 α is a chemokine, strongly induced in an inflammatory setting [54]. It is known to be a
325 powerful chemoattractant for CXCR4-expressing stem cell populations as well as bone marrow-
326 derived immune cells [33, 54, 55]. As such, SDF-1 α was shown to be a potent chemoattractant of
327 inflammatory monocytes *in vivo*, greater even than action of monocyte chemoattractant protein-1
328 (MCP-1)[33]. Various cancers use the SDF-1 α /CXCR4 signaling axis to recruit inflammatory
329 macrophages to the tissues [56, 57]. In a model of spinal cord injury, locally expressed SDF-1 α
330 in conjunction with matrix metalloproteinase-9 supports the migration of monocytes into the
331 injured spinal cord [31]. Another recent report provides compelling evidence that the CXCR7
332 receptor is induced during monocyte-to-macrophage transition and is expressed at higher levels
333 on M1 macrophages. Therefore, in addition to promoting macrophage recruitment, SDF-1 α
334 signals via CXCR7 to enhance macrophage phagocytosis, contributing to pathogenesis of
335 atherosclerosis [58]. Myocardial CXCR4 overexpression led to the exacerbation of I/R injury in
336 the heart by increasing inflammatory infiltrate [59], while transendocardial delivery of SDF-1 α
337 failed to improve myocardial perfusion and ventricular function [60]. These studies suggest that
338 exaggerated signaling via SDF-1 α -CXCR4/7 axis may lead to detrimental effects on tissue
339 regeneration especially during early stages of muscle regeneration where efficient resolution of
340 the inflammatory response is required for the timely onset of tissue repair [61, 62].

341 In our model of TK-I/R injury, tissue necrosis, vascular damage, severe inflammation and
342 functional deficits are the hallmarks of I/R-induced muscle pathology [2, 63]. It is established
343 that inflammatory monocytes/macrophages (M1) are recruited early in regeneration and,
344 although, absolutely required for the clearance of necrotic debris at the site of injury, their
345 persistence often exacerbates inflammation and delays regeneration [64-66]. Muscle fiber
346 necrosis following I/R injury is a potent pro-inflammatory activator of recruited monocytes [67].
347 Recently, high mobility group box-1, a nuclear protein released by necrotic cells, was shown to
348 form a hetero-complex with SDF-1 α and act via CXCR4 to recruit inflammatory cells [68]. I/R-
349 induced muscle necrosis combined with progressive release of SDF-1 α from PEG-Fib matrix in
350 our injury model may have contributed to the recruitment of additional inflammatory CXCR4⁺
351 cells prolonging local inflammation and delaying onset of muscle regeneration.
352 Immunofluorescence data showing increased numbers of CXCR4⁺ cells in muscles treated with
353 PEG-Fib/SDF-1 α late in regeneration response serve as evidence of either ongoing cell
354 recruitment or local proliferation, both of which are characteristics of early phase regenerative
355 events [69].

356 In literature, the beneficial role of SDF-1 α is associated with improved restoration of ischemic
357 tissue perfusion and neovascularization [40]. Several reports mention SDF-1 α -recruited
358 CXCR4⁺CD11b⁺ cells as primary mediators of neovascularization [37]. Multiple solid tumors
359 exploit the SDF-1 α /CXCR4 axis for the recruitment of M1 macrophages to promote and support
360 the establishment of the vascular supply for tumor survival. As such, in a highly inflammatory
361 context, a pro-angiogenic environment leads to the formation of immature and fragile neovessels.
362 The recruitment of CD34⁺ endothelial progenitor cells via the SDF-1 α /CXCR4 signaling axis
363 may contribute to inflammatory angiogenesis [23]. In our model, both groups treated with SDF-

364 1α showed significantly enhanced muscle revascularization/neovascularization, even when
365 compared with uninjured control. However, administration of PEG-Fib/SDF- 1α often resulted in
366 leakage of blood throughout the muscle (data not shown), which can be a consequence of
367 rupture, permeability and lack of stability of newly formed microvasculature in this group. The
368 abundance of small myofibers and the persistence of CXCR4⁺ cells at the site of injury as late as
369 two weeks post-reperfusion provide further evidence for the ongoing degeneration/regeneration
370 sequence of events. Increased collagen deposition in PEG-Fib and PEG-Fib/SDF- 1α treated
371 muscles may be indicative of M2 macrophage activity in the inflammatory setting [70]. These
372 cells appear in the muscles as early as 3 days post-reperfusion [71] and produce arginase-1 and
373 TGF- β factors both of which contribute to extracellular matrix deposition [72]. Overall, there
374 appears to be no functional benefit from SDF- 1α treatment up to 14 days post-TK-I/R injury
375 compared to matrix delivery alone, despite apparent enhancement in neovascularization.

376 Interestingly, in the combined delivery of PEG-Fib/SDF- 1α /IGF-I, IGF-I was able to
377 complement the SDF- 1α -mediated neovascularization effect. Muscles treated with PEG-Fib
378 matrix containing both SDF- 1α and IGF-I showed enhanced revascularization, increased
379 myofiber distribution, decreased fibrosis and enhanced contractile function when compared to
380 PEG-Fib matrix delivery alone. Our group has previously shown significant beneficial effects of
381 PEG-Fib/IGF-I administration on muscle recovery following TK-I/R injury. It was apparent that
382 functional improvements using PEG-Fib/SDF- 1α /IGF-I therapy were very similar to functional
383 recovery using PEG-Fib/IGF-I therapy of TK-I/R injured muscles [28]. Therefore, we concluded
384 that beneficial effects of PEG-Fib/SDF- 1α /IGF-I therapy on restoration of muscle contractile
385 function are primarily attributed to IGF-I activity, a potent anti-inflammatory, pro-regenerative,
386 anti-apoptotic and hypertrophy-promoting growth factor [42]. In order to better understand the

387 effect of exogenous SDF-1 α delivery on muscle regeneration, we need to perform additional
388 functional testing to evaluate the benefit of enhanced vascularization on restoration of work
389 capacity in PEG-Fib/SDF-1 α /IGF-I treatment group, as well as characterize and quantify SDF-
390 1 α -mediated effects on inflammatory and precursor cells recruitment at the early stages of
391 muscle regeneration.

392 The release kinetics of SDF-1 α /IGF-I from PEG-Fib matrix were previously evaluated by our
393 group as well as Zhang et al [29]. Sequence of factor release at the site of acute injury may be
394 responsible for the therapeutic effect seen after dual PEG-Fib/SDF-1 α /IGF-I delivery. The
395 majority of IGF-I is released from the matrix within the first 24 hours and at physiologically
396 relevant levels over a 4-day period, while slightly larger SDF-I is progressively released over 7
397 days. The powerful anti-inflammatory, pro-regenerative signal delivered via IGF-I may have
398 inhibited SDF-1-dependent inflammatory cell recruitment at the later stages of muscle
399 regeneration and/or facilitated earlier inflammatory resolution and onset of tissue repair. Future
400 studies should address how changing the order and kinetics of SDF-1 α /IGF-I release may impact
401 functional tissue regeneration.

402 **CONCLUSION**

403 We did not observe functional improvements after PEG-Fib/SDF-1 α treatment, despite
404 treatment-induced increase in persistence of CXCR4⁺ cells and enhanced tissue revascularization
405 at two weeks after initial injury. Functional analysis showed no significant difference in maximal
406 force recovery between matrix alone treatment and addition of SDF-1 α . As expected, combined
407 PEG-Fib/SDF-1 α /IGF-I delivery in addition to enhanced revascularization, significantly
408 improved functional recovery following TK-I/R. However, the effect of combined PEG-

409 Fib/SDF-1 α /IGF-I therapy on recovery of muscle force appeared to be IGF-I mediated. Our data
410 confirm the requirement for IGF-I in promoting muscle repair and pro-angiogenic effects of
411 SDF-1 α on tissue revascularization. We did not show beneficial effects of SDF-1 α treatment on
412 contractile force recovery at 14 days after TK-I/R injury. Nevertheless, combined growth factor
413 therapy can offer multiple benefits provided that one can manipulate the release order, kinetics
414 and gradients of delivered mediators in the microenvironment in spatiotemporal manner to
415 promote efficient repair.

416 REFERENCES

- 417
- 418 [1] Vignaud A, Hourde C, Medja F, Agbulut O, Butler-Browne G, Ferry A. Impaired skeletal
419 muscle repair after ischemia-reperfusion injury in mice. *Journal of biomedicine &*
420 *biotechnology*. 2010;2010:724914.
- 421 [2] Hammers DW, Merritt EK, Matheny RW, Jr., Adamo ML, Walters TJ, Estep JS, et al.
422 Functional deficits and insulin-like growth factor-I gene expression following tourniquet-induced
423 injury of skeletal muscle in young and old rats. *Journal of applied physiology*. 2008;105:1274-
424 81.
- 425 [3] Ceafalan LC, Popescu BO, Hinescu ME. Cellular players in skeletal muscle regeneration.
426 *BioMed research international*. 2014;2014:957014.
- 427 [4] Jeong J, Shin K, Lee SB, Lee DR, Kwon H. Patient-tailored application for Duchene
428 muscular dystrophy on mdx mice based induced mesenchymal stem cells. *Experimental and*
429 *molecular pathology*. 2014;97:253-8.

- 430 [5] Meregalli M, Farini A, Sitzia C, Torrente Y. Advancements in stem cells treatment of
431 skeletal muscle wasting. *Frontiers in physiology*. 2014;5:48.
- 432 [6] Wang YX, Dumont NA, Rudnicki MA. Muscle stem cells at a glance. *Journal of cell science*.
433 2014;127:4543-8.
- 434 [7] Tedesco FS, Cossu G. Stem cell therapies for muscle disorders. *Current opinion in neurology*.
435 2012;25:597-603.
- 436 [8] Usas A, Maciulaitis J, Maciulaitis R, Jakuboniene N, Milasius A, Huard J. Skeletal muscle-
437 derived stem cells: implications for cell-mediated therapies. *Medicina*. 2011;47:469-79.
- 438 [9] Meng J, Adkin CF, Arechavala-Gomez V, Boldrin L, Muntoni F, Morgan JE. The
439 contribution of human synovial stem cells to skeletal muscle regeneration. *Neuromuscular*
440 *disorders : NMD*. 2010;20:6-15.
- 441 [10] Boldrin L, Morgan JE. Activating muscle stem cells: therapeutic potential in muscle
442 diseases. *Current opinion in neurology*. 2007;20:577-82.
- 443 [11] Liew A, O'Brien T. Therapeutic potential for mesenchymal stem cell transplantation in
444 critical limb ischemia. *Stem cell research & therapy*. 2012;3:28.
- 445 [12] Corona BT, Rathbone CR. Accelerated functional recovery after skeletal muscle ischemia-
446 reperfusion injury using freshly isolated bone marrow cells. *The Journal of surgical research*.
447 2014;188:100-9.

- 448 [13] Corona BT, Wenke JC, Walters TJ, Rathbone CR. Intramuscular transplantation and
449 survival of freshly isolated bone marrow cells following skeletal muscle ischemia-reperfusion
450 injury. *The journal of trauma and acute care surgery*. 2013;75:S142-9.
- 451 [14] Quattrocelli M, Cassano M, Crippa S, Perini I, Sampaolesi M. Cell therapy strategies and
452 improvements for muscular dystrophy. *Cell death and differentiation*. 2010;17:1222-9.
- 453 [15] Viswanathan S, Keating A, Deans R, Hematti P, Prockop D, Stroncek DF, et al. Soliciting
454 strategies for developing cell-based reference materials to advance mesenchymal stromal cell
455 research and clinical translation. *Stem cells and development*. 2014;23:1157-67.
- 456 [16] Rosland GV, Svendsen A, Torsvik A, Sobala E, McCormack E, Immervoll H, et al. Long-
457 term cultures of bone marrow-derived human mesenchymal stem cells frequently undergo
458 spontaneous malignant transformation. *Cancer research*. 2009;69:5331-9.
- 459 [17] Eggenhofer E, Benseler V, Kroemer A, Popp FC, Geissler EK, Schlitt HJ, et al.
460 Mesenchymal stem cells are short-lived and do not migrate beyond the lungs after intravenous
461 infusion. *Frontiers in immunology*. 2012;3:297.
- 462 [18] Iso Y, Spees JL, Serrano C, Bakondi B, Pochampally R, Song YH, et al. Multipotent human
463 stromal cells improve cardiac function after myocardial infarction in mice without long-term
464 engraftment. *Biochemical and biophysical research communications*. 2007;354:700-6.
- 465 [19] Prockop DJ, Oh JY. Mesenchymal stem/stromal cells (MSCs): role as guardians of
466 inflammation. *Molecular therapy : the journal of the American Society of Gene Therapy*.
467 2012;20:14-20.

- 468 [20] Chen XK, Rathbone CR, Walters TJ. Treatment of tourniquet-induced ischemia reperfusion
469 injury with muscle progenitor cells. *The Journal of surgical research*. 2011;170:e65-73.
- 470 [21] Ota S, Uehara K, Nozaki M, Kobayashi T, Terada S, Tobita K, et al. Intramuscular
471 transplantation of muscle-derived stem cells accelerates skeletal muscle healing after contusion
472 injury via enhancement of angiogenesis. *The American journal of sports medicine*.
473 2011;39:1912-22.
- 474 [22] Bencze M, Negroni E, Vallese D, Yacoub-Youssef H, Chaouch S, Wolff A, et al.
475 Proinflammatory macrophages enhance the regenerative capacity of human myoblasts by
476 modifying their kinetics of proliferation and differentiation. *Molecular therapy : the journal of*
477 *the American Society of Gene Therapy*. 2012;20:2168-79.
- 478 [23] Kuliszewski MA, Kobulnik J, Lindner JR, Stewart DJ, Leong-Poi H. Vascular gene transfer
479 of SDF-1 promotes endothelial progenitor cell engraftment and enhances angiogenesis in
480 ischemic muscle. *Molecular therapy : the journal of the American Society of Gene Therapy*.
481 2011;19:895-902.
- 482 [24] Borselli C, Storrie H, Benesch-Lee F, Shvartsman D, Cezar C, Lichtman JW, et al.
483 Functional muscle regeneration with combined delivery of angiogenesis and myogenesis factors.
484 *Proceedings of the National Academy of Sciences of the United States of America*.
485 2010;107:3287-92.
- 486 [25] Kuraitis D, Zhang P, Zhang Y, Padavan DT, McEwan K, Sofrenovic T, et al. A stromal cell-
487 derived factor-1 releasing matrix enhances the progenitor cell response and blood vessel growth
488 in ischaemic skeletal muscle. *European cells & materials*. 2011;22:109-23.

- 489 [26] Thevenot PT, Nair AM, Shen J, Lotfi P, Ko CY, Tang L. The effect of incorporation of
490 SDF-1alpha into PLGA scaffolds on stem cell recruitment and the inflammatory response.
491 Biomaterials. 2010;31:3997-4008.
- 492 [27] Drinnan CT, Zhang G, Alexander MA, Pulido AS, Suggs LJ. Multimodal release of
493 transforming growth factor-beta1 and the BB isoform of platelet derived growth factor from
494 PEGylated fibrin gels. Journal of controlled release : official journal of the Controlled Release
495 Society. 2010;147:180-6.
- 496 [28] Hammers DW, Sarathy A, Pham CB, Drinnan CT, Farrar RP, Suggs LJ. Controlled release
497 of IGF-I from a biodegradable matrix improves functional recovery of skeletal muscle from
498 ischemia/reperfusion. Biotechnology and bioengineering. 2012;109:1051-9.
- 499 [29] Zhang G, Nakamura Y, Wang X, Hu Q, Suggs LJ, Zhang J. Controlled release of stromal
500 cell-derived factor-1 alpha in situ increases c-kit+ cell homing to the infarcted heart. Tissue
501 engineering. 2007;13:2063-71.
- 502 [30] Ho TK, Tsui J, Xu S, Leoni P, Abraham DJ, Baker DM. Angiogenic effects of stromal cell-
503 derived factor-1 (SDF-1/CXCL12) variants in vitro and the in vivo expressions of CXCL12
504 variants and CXCR4 in human critical leg ischemia. Journal of vascular surgery. 2010;51:689-
505 99.
- 506 [31] Zhang H, Trivedi A, Lee JU, Lohela M, Lee SM, Fandel TM, et al. Matrix
507 metalloproteinase-9 and stromal cell-derived factor-1 act synergistically to support migration of
508 blood-borne monocytes into the injured spinal cord. The Journal of neuroscience : the official
509 journal of the Society for Neuroscience. 2011;31:15894-903.

- 510 [32] Aiuti A, Webb IJ, Bleul C, Springer T, Gutierrez-Ramos JC. The chemokine SDF-1 is a
511 chemoattractant for human CD34+ hematopoietic progenitor cells and provides a new
512 mechanism to explain the mobilization of CD34+ progenitors to peripheral blood. *The Journal of*
513 *experimental medicine*. 1997;185:111-20.
- 514 [33] Bleul CC, Fuhlbrigge RC, Casasnovas JM, Aiuti A, Springer TA. A highly efficacious
515 lymphocyte chemoattractant, stromal cell-derived factor 1 (SDF-1). *The Journal of experimental*
516 *medicine*. 1996;184:1101-9.
- 517 [34] Hamed S, Egozi D, Dawood H, Keren A, Kruchevsky D, Ben-Nun O, et al. The chemokine
518 stromal cell-derived factor-1 α promotes endothelial progenitor cell-mediated
519 neovascularization of human transplanted fat tissue in diabetic immunocompromised mice.
520 *Plastic and reconstructive surgery*. 2013;132:239e-50e.
- 521 [35] Ziaei R, Ayatollahi M, Yaghobi R, Sahraeian Z, Zarghami N. Involvement of TNF- α in
522 differential gene expression pattern of CXCR4 on human marrow-derived mesenchymal stem
523 cells. *Molecular biology reports*. 2014;41:1059-66.
- 524 [36] Ratajczak MZ, Majka M, Kucia M, Drukala J, Pietrzkowski Z, Peiper S, et al. Expression of
525 functional CXCR4 by muscle satellite cells and secretion of SDF-1 by muscle-derived fibroblasts
526 is associated with the presence of both muscle progenitors in bone marrow and hematopoietic
527 stem/progenitor cells in muscles. *Stem cells*. 2003;21:363-71.
- 528 [37] Wragg A, Mellad JA, Beltran LE, Konoplyannikov M, San H, Boozer S, et al.
529 VEGFR1/CXCR4-positive progenitor cells modulate local inflammation and augment tissue
530 perfusion by a SDF-1-dependent mechanism. *Journal of molecular medicine*. 2008;86:1221-32.

- 531 [38] Stokman G, Stroo I, Claessen N, Teske GJ, Florquin S, Leemans JC. SDF-1 provides
532 morphological and functional protection against renal ischaemia/reperfusion injury. *Nephrology,*
533 *dialysis, transplantation : official publication of the European Dialysis and Transplant*
534 *Association - European Renal Association.* 2010;25:3852-9.
- 535 [39] Stroo I, Stokman G, Teske GJ, Florquin S, Leemans JC. Haematopoietic stem cell migration
536 to the ischemic damaged kidney is not altered by manipulating the SDF-1/CXCR4-axis.
537 *Nephrology, dialysis, transplantation : official publication of the European Dialysis and*
538 *Transplant Association - European Renal Association.* 2009;24:2082-8.
- 539 [40] Ghadge SK, Muhlstedt S, Ozcelik C, Bader M. SDF-1alpha as a therapeutic stem cell
540 homing factor in myocardial infarction. *Pharmacology & therapeutics.* 2011;129:97-108.
- 541 [41] Florini JR, Ewton DZ, Coolican SA. Growth hormone and the insulin-like growth factor
542 system in myogenesis. *Endocrine reviews.* 1996;17:481-517.
- 543 [42] Pelosi L, Giacinti C, Nardis C, Borsellino G, Rizzuto E, Nicoletti C, et al. Local expression
544 of IGF-1 accelerates muscle regeneration by rapidly modulating inflammatory cytokines and
545 chemokines. *FASEB journal : official publication of the Federation of American Societies for*
546 *Experimental Biology.* 2007;21:1393-402.
- 547 [43] Coleman ME, DeMayo F, Yin KC, Lee HM, Geske R, Montgomery C, et al. Myogenic
548 vector expression of insulin-like growth factor I stimulates muscle cell differentiation and
549 myofiber hypertrophy in transgenic mice. *The Journal of biological chemistry.* 1995;270:12109-
550 16.

551 [44] Adams GR, McCue SA. Localized infusion of IGF-I results in skeletal muscle hypertrophy
552 in rats. *J Appl Physiol* (1985). 1998;84:1716-22.

553 [45] Lee S, Barton ER, Sweeney HL, Farrar RP. Viral expression of insulin-like growth factor-I
554 enhances muscle hypertrophy in resistance-trained rats. *Journal of applied physiology*.
555 2004;96:1097-104.

556 [46] Musaro A, McCullagh K, Paul A, Houghton L, Dobrowolny G, Molinaro M, et al.
557 Localized Igf-1 transgene expression sustains hypertrophy and regeneration in senescent skeletal
558 muscle. *Nature genetics*. 2001;27:195-200.

559 [47] Chakravarthy MV, Booth FW, Spangenburg EE. The molecular responses of skeletal
560 muscle satellite cells to continuous expression of IGF-1: implications for the rescue of induced
561 muscular atrophy in aged rats. *International journal of sport nutrition and exercise metabolism*.
562 2001;11 Suppl:S44-8.

563 [48] Merritt EK, Hammers DW, Tierney M, Suggs LJ, Walters TJ, Farrar RP. Functional
564 assessment of skeletal muscle regeneration utilizing homologous extracellular matrix as
565 scaffolding. *Tissue engineering Part A*. 2010;16:1395-405.

566 [49] Hammers DW, Matheny RW, Jr., Sell C, Adamo ML, Walters TJ, Estep JS, et al.
567 Impairment of IGF-I expression and anabolic signaling following ischemia/reperfusion in
568 skeletal muscle of old mice. *Experimental gerontology*. 2011;46:265-72.

569 [50] Cencioni C, Capogrossi MC, Napolitano M. The SDF-1/CXCR4 axis in stem cell
570 preconditioning. *Cardiovascular research*. 2012;94:400-7.

- 571 [51] Mirshahi F, Pourtau J, Li H, Muraine M, Trochon V, Legrand E, et al. SDF-1 activity on
572 microvascular endothelial cells: consequences on angiogenesis in in vitro and in vivo models.
573 *Thrombosis research*. 2000;99:587-94.
- 574 [52] Cavalera M, Frangogiannis NG. Targeting the chemokines in cardiac repair. *Current*
575 *pharmaceutical design*. 2014;20:1971-9.
- 576 [53] Moyer AL, Wagner KR. Regeneration versus fibrosis in skeletal muscle. *Current opinion in*
577 *rheumatology*. 2011;23:568-73.
- 578 [54] Kucia M, Jankowski K, Reza R, Wysoczynski M, Bandura L, Allendorf DJ, et al. CXCR4-
579 SDF-1 signalling, locomotion, chemotaxis and adhesion. *Journal of molecular histology*.
580 2004;35:233-45.
- 581 [55] Kucia M, Ratajczak J, Ratajczak MZ. Bone marrow as a source of circulating CXCR4+
582 tissue-committed stem cells. *Biology of the cell / under the auspices of the European Cell*
583 *Biology Organization*. 2005;97:133-46.
- 584 [56] Schmid MC, Avraamides CJ, Foubert P, Shaked Y, Kang SW, Kerbel RS, et al. Combined
585 blockade of integrin- $\alpha 4 \beta 1$ plus cytokines SDF-1 α or IL-1 β potently inhibits tumor
586 inflammation and growth. *Cancer research*. 2011;71:6965-75.
- 587 [57] Tseng D, Vasquez-Medrano DA, Brown JM. Targeting SDF-1/CXCR4 to inhibit tumour
588 vasculature for treatment of glioblastomas. *British journal of cancer*. 2011;104:1805-9.

- 589 [58] Ma W, Liu Y, Ellison N, Shen J. Induction of C-X-C chemokine receptor type 7 (CXCR7)
590 switches stromal cell-derived factor-1 (SDF-1) signaling and phagocytic activity in macrophages
591 linked to atherosclerosis. *The Journal of biological chemistry*. 2013;288:15481-94.
- 592 [59] Chen J, Chemaly E, Liang L, Kho C, Lee A, Park J, et al. Effects of CXCR4 gene transfer
593 on cardiac function after ischemia-reperfusion injury. *The American journal of pathology*.
594 2010;176:1705-15.
- 595 [60] Koch KC, Schaefer WM, Liehn EA, Rammos C, Mueller D, Schroeder J, et al. Effect of
596 catheter-based transendocardial delivery of stromal cell-derived factor 1alpha on left ventricular
597 function and perfusion in a porcine model of myocardial infarction. *Basic research in cardiology*.
598 2006;101:69-77.
- 599 [61] Nathan C. Points of control in inflammation. *Nature*. 2002;420:846-52.
- 600 [62] Wang H, Melton DW, Porter L, Sarwar ZU, McManus LM, Shireman PK. Altered
601 macrophage phenotype transition impairs skeletal muscle regeneration. *The American journal of*
602 *pathology*. 2014;184:1167-84.
- 603 [63] Blaisdell FW. The pathophysiology of skeletal muscle ischemia and the reperfusion
604 syndrome: a review. *Cardiovascular surgery*. 2002;10:620-30.
- 605 [64] Mounier R, Theret M, Arnold L, Cuvellier S, Bultot L, Goransson O, et al. AMPKalpha1
606 Regulates Macrophage Skewing at the Time of Resolution of Inflammation during Skeletal
607 Muscle Regeneration. *Cell metabolism*. 2013;18:251-64.

- 608 [65] Tidball JG. Inflammatory processes in muscle injury and repair. *American journal of*
609 *physiology Regulatory, integrative and comparative physiology*. 2005;288:R345-53.
- 610 [66] Tidball JG. Inflammatory cell response to acute muscle injury. *Medicine and science in*
611 *sports and exercise*. 1995;27:1022-32.
- 612 [67] Brechot N, Gomez E, Bignon M, Khallou-Laschet J, Dussiot M, Cazes A, et al. Modulation
613 of macrophage activation state protects tissue from necrosis during critical limb ischemia in
614 thrombospondin-1-deficient mice. *PloS one*. 2008;3:e3950.
- 615 [68] Schiraldi M, Raucci A, Munoz LM, Livoti E, Celona B, Venereau E, et al. HMGB1
616 promotes recruitment of inflammatory cells to damaged tissues by forming a complex with
617 CXCL12 and signaling via CXCR4. *The Journal of experimental medicine*. 2012;209:551-63.
- 618 [69] Hawke TJ, Garry DJ. Myogenic satellite cells: physiology to molecular biology. *J Appl*
619 *Physiol* (1985). 2001;91:534-51.
- 620 [70] Wang Y, Wehling-Henricks M, Samengo G, Tidball JG. Increases of M2a macrophages and
621 fibrosis in aging muscle are influenced by bone marrow aging and negatively regulated by
622 muscle-derived nitric oxide. *Aging cell*. 2015.
- 623 [71] Hammers DW, Rybalko V, Merscham-Banda M, Hsieh PL, Suggs LJ, Farrar RP. Anti-
624 inflammatory macrophages improve skeletal muscle recovery from ischemia/reperfusion. *J Appl*
625 *Physiol* (1985). 2015:jap 00313 2014.
- 626 [72] Novak ML, Koh TJ. Macrophage phenotypes during tissue repair. *Journal of leukocyte*
627 *biology*. 2013;93:875-81.

1 **FIGURE CAPTIONS**

2

3 **Figure 1.** Western blots showing the binding of SDF-1 α and IGF-I to conjugated poly(ethylene
4 glycol) (PEG) fibrinogen (Fib). **Lane 1:** recombinant rat SDF-1 α (20 μ g/ml) (top), recombinant
5 human IGF-I (50 μ g/ml) (bottom); **Lane 2:** Fibrinogen (10 mg/ml); **Lane 3:** PEGylated
6 fibrinogen; **Lane 4:** PEGylated fibrinogen/SDF-1 α /IGF-I probed against SDF-1 α (top) and IGF-I
7 (bottom) \geq 60kDa in size. Final concentrations of SDF-1 α and IGF-I following PEGylation
8 were 10 μ g/ml and 25 μ g/ml respectively.

9

10 **Figure 2.** Quantification of CXCR4⁺ cells within I/R injured skeletal muscle 14 days post-
11 reperfusion. Animals were treated with PEGylated fibrin (PEG-Fib), PEGylated fibrin
12 conjugated to SDF-1 α (PEG-Fib/SDF-1 α), PEGylated fibrin conjugated to IGF-I (PEG-Fib/ IGF-
13 I), and PEGylated fibrin conjugated to SDF-1 α and IGF-I (PEG-Fib/SDF-1 α /IGF-I) 24h after
14 TK-I/R injury and analyzed 14 days post-reperfusion. Contralateral control (n=5, 3 fields of
15 view/animal); TK-I/R (n=6, 3 fields of view/animal). Values expressed as mean \pm SEM, one-way
16 ANOVA, Tukey post-hoc: * p<0.05 versus PEG-Fib, # p<0.05 PEG-Fib/SDF-1 α versus PEG-
17 Fib/SDF-1 α /IGF-I.

18

19 **Figure 3.** Identification and quantification of CD31⁺ cells within I/R injured skeletal muscle 14
20 days post-reperfusion. Animals were treated with PEGylated fibrin (PEG-Fib), PEGylated fibrin
21 conjugated to SDF-1 α (PEG-Fib/SDF-1 α), PEGylated fibrin conjugated to IGF-I (PEG-Fib/ IGF-
22 I), and PEGylated fibrin conjugated to SDF-1 α and IGF-I (PEG-Fib/SDF-1 α /IGF-I) 24h after
23 TK-I/R injury and analyzed 14 days post-reperfusion. Representative images of CD31⁺ staining
24 (200X) and quantification of CD31⁺ cells/muscle fiber (n=3, 3 fields of view/animal). Values

25 expressed as mean \pm SEM, one-way ANOVA, Tukey post-hoc: * $p < 0.05$ versus uninjured control,
26 # $p < 0.05$ versus PEG-Fib group, [†] $p < 0.05$ versus PEG-Fib/SDF-1 α group.

27

28 **Figure 4.** Percent maximum force production recovery among treatment groups 14 days after I/R
29 injury. Maximum tetanic force production (P_0) of the LGAS was measured *in situ* from the
30 following groups: PEGylated fibrin (PEG-Fib), PEGylated fibrin conjugated to SDF-1 α (PEG-
31 Fib/SDF-1), and PEGylated fibrin conjugated to SDF-1 α and IGF-I (PEG-Fib/SDF-1 α /IGF-I).
32 The P_0 were compared to the contralateral leg that received no injury. Values expressed as mean
33 \pm SEM, one-way ANOVA, Tukey post-hoc: * $p < 0.05$ versus PEG-Fib, $n = 6$.

34

35

36 **Figure 5.** Functional recovery of tetanic tension among treatment groups 14 days after I/R
37 injury. Specific tension (SP_0) of the LGAS was measured *in situ* for the following groups:
38 PEGylated fibrin (PEG-Fib), PEGylated fibrin conjugated to SDF-1 α (PEG-Fib/SDF-1), and
39 PEGylated fibrin conjugated to SDF-1 α and IGF-I (PEG-Fib/SDF-1/IGF-I). Values expressed as
40 mean \pm SEM, one-way ANOVA, Tukey post-hoc: [†] $p < 0.05$ versus uninjured, * $p < 0.05$ versus
41 PEG-Fib, # $p < 0.05$ versus PEG-Fib/SDF-1, $n = 6$

42

43 **Figure 6.** Histological analysis of I/R injured skeletal muscle 14 days post-reperfusion. H&E
44 stained sections were examined for fiber size distribution (200X). Data expressed as percent
45 myofibers of a given area (μm^2). Representative images are included: (A) PEGylated fibrin
46 (PEG-Fib), (B) PEGylated fibrin conjugated to SDF-1 α (PEG-Fib/SDF-1 α), (C) PEGylated
47 fibrin conjugated to SDF-1 α and IGF-I (PEG-Fib/SDF-1 α /IGF-I).

48

49 **Figure 7.** Quantification of collagen deposition in I/R injured skeletal muscle 14 days post-
50 reperfusion. Animals were treated with PEGylated fibrin (PEG-Fib), PEGylated fibrin
51 conjugated to SDF-1 α (PEG-Fib/SDF-1 α), and PEGylated fibrin conjugated to SDF-1 α and IGF-
52 I (PEG-Fib/SDF-1 α /IGF-I) 24h after TK-I/R injury and analyzed 14 days post-reperfusion.
53 Representative images of trichrome staining (200X) where collagen staining is shown in blue
54 (n=3, 3 fields of view/animal). Values expressed as mean \pm SEM, one-way ANOVA, Tukey post-
55 hoc: * p<0.05 versus PEG-Fib group.

56

57

58

59

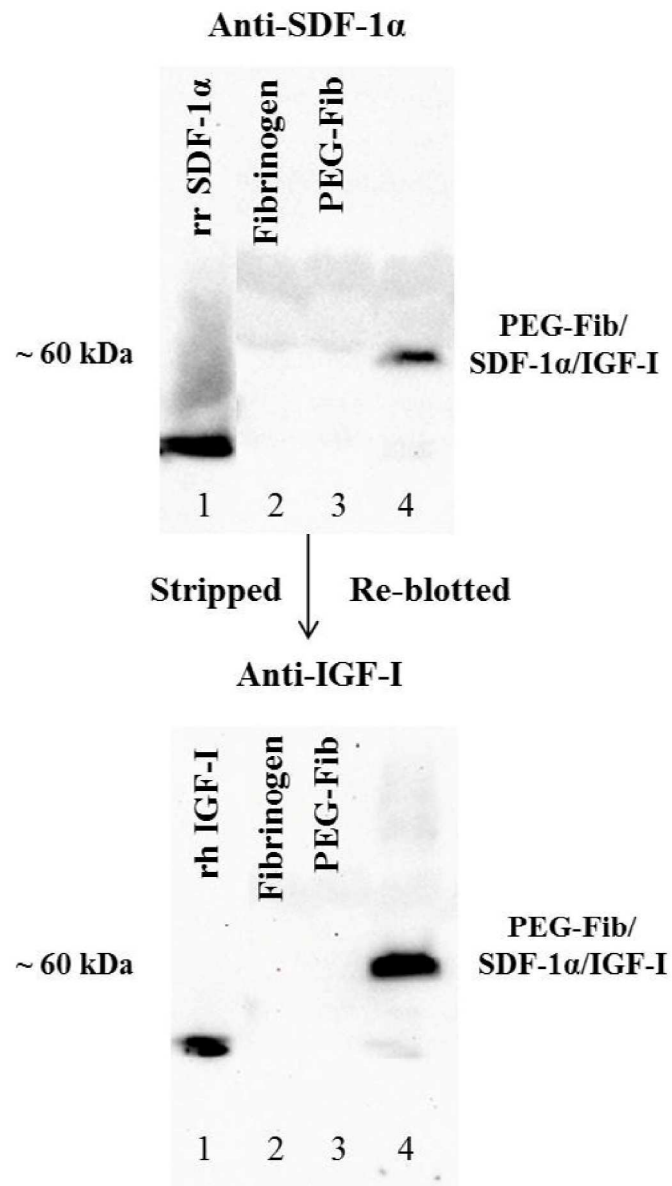


Figure 1. Western blots showing the binding of SDF-1 α and IGF-I to conjugated poly(ethylene glycol) (PEG) fibrinogen (Fib). Lane 1: recombinant rat SDF-1 α (20 μ g/ml) (top), recombinant human IGF-I (50 μ g/ml) (bottom); Lane 2: Fibrinogen (10 mg/ml); Lane 3: PEGylated fibrinogen; Lane 4: PEGylated fibrinogen/SDF-1 α /IGF-I probed against SDF-1 α (top) and IGF-I (bottom) \geq 60kDa in size. Final concentrations of SDF-1 α and IGF-I following PEGylation were 10 μ g/ml and 25 μ g/ml respectively.
279x431mm (300 x 300 DPI)

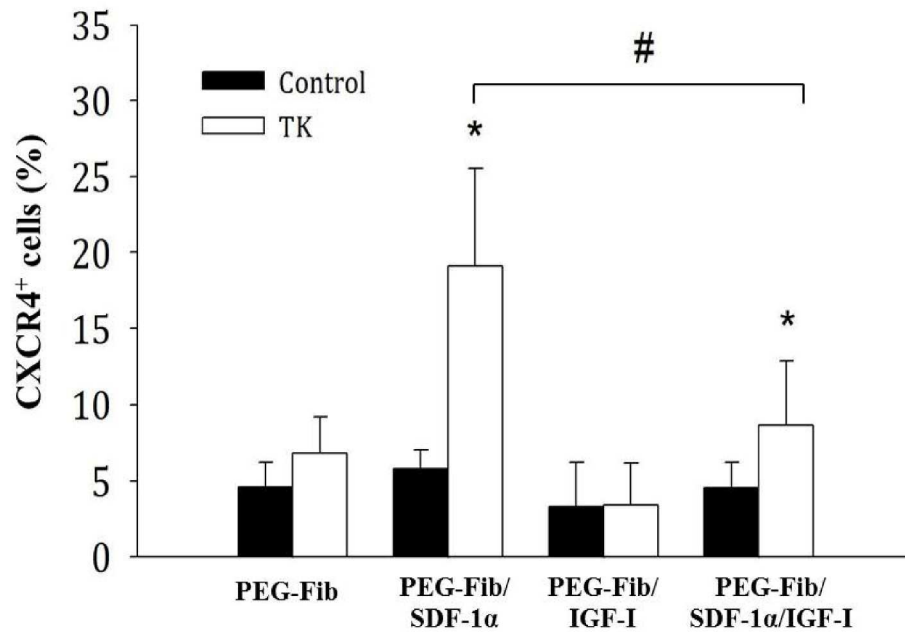


Figure 2. Quantification of CXCR4⁺ cells within I/R injured skeletal muscle 14 days post-reperfusion. Animals were treated with PEGylated fibrin (PEG-Fib), PEGylated fibrin conjugated to SDF-1 α (PEG-Fib/SDF-1 α), PEGylated fibrin conjugated to IGF-I (PEG-Fib/IGF-I), and PEGylated fibrin conjugated to SDF-1 α and IGF-I (PEG-Fib/SDF-1 α /IGF-I) 24h after TK-I/R injury and analyzed 14 days post-reperfusion. Contralateral control (n=5, 3 fields of view/animal); TK-I/R (n=6, 3 fields of view/animal). Values expressed as mean \pm SEM, one-way ANOVA, Tukey post-hoc: *p<0.05 versus PEG-Fib, # p<0.05 PEG-Fib/SDF-1 α versus PEG-Fib/SDF-1 α /IGF-I.

279x215mm (300 x 300 DPI)

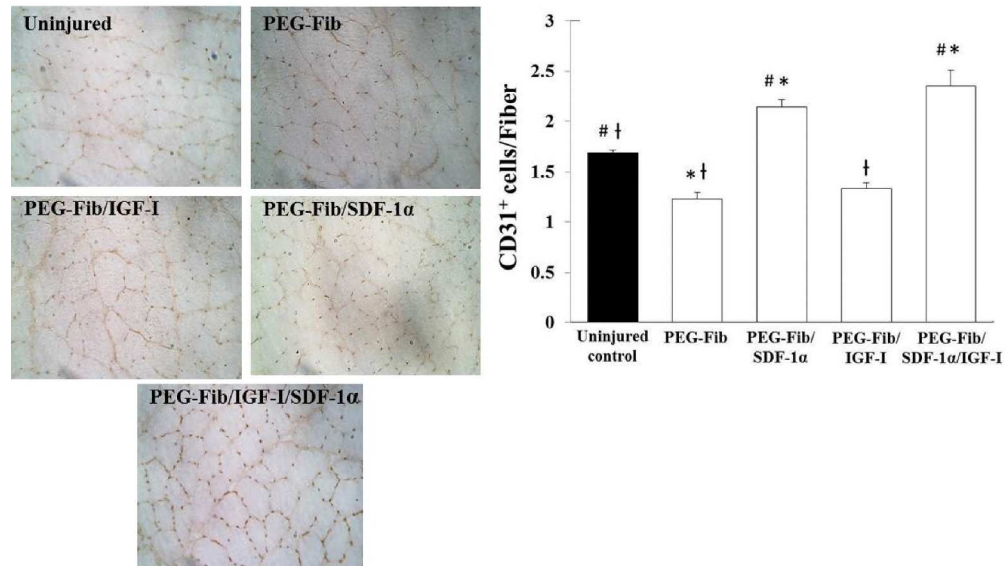


Figure 3. Identification and quantification of CD31⁺ cells within I/R injured skeletal muscle 14 days post-reperfusion. Animals were treated with PEGylated fibrin (PEG-Fib), PEGylated fibrin conjugated to SDF-1α (PEG-Fib/SDF-1α), PEGylated fibrin conjugated to IGF-I (PEG-Fib/IGF-I), and PEGylated fibrin conjugated to SDF-1α and IGF-I (PEG-Fib/SDF-1α/IGF-I) 24h after TK-I/R injury and analyzed 14 days post-reperfusion. Representative images of CD31⁺ staining (200X) and quantification of CD31⁺ cells/muscle fiber (n=3, 3 fields of view/animal). Values expressed as mean ± SEM, one-way ANOVA, Tukey post-hoc: * p<0.05 versus uninjured control, # p<0.05 versus PEG-Fib group, † p<0.05 versus PEG-Fib/SDF-1α group. 279x215mm (300 x 300 DPI)

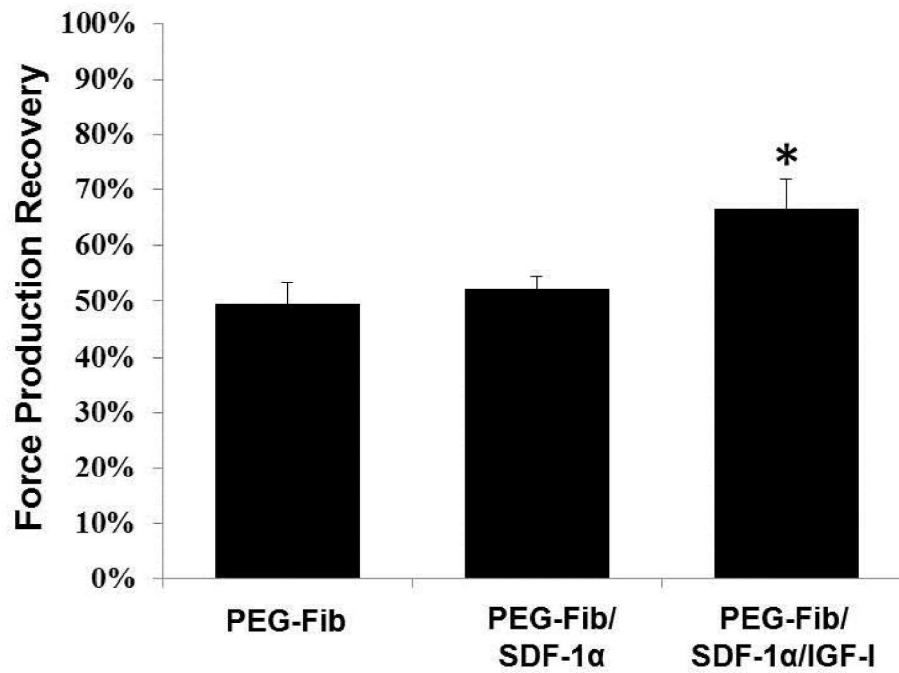


Figure 4. Percent maximum force production recovery among treatment groups 14 days after I/R injury. Maximum tetanic force production (P0) of the LGAS was measured in situ from the following groups: PEGylated fibrin (PEG-Fib), PEGylated fibrin conjugated to SDF-1 α (PEG-Fib/SDF-1), and PEGylated fibrin conjugated to SDF-1 α and IGF-I (PEG-Fib/SDF-1 α /IGF-I). The P0 were compared to the contralateral leg that received no injury. Values expressed as mean \pm SEM, one-way ANOVA, Tukey post-hoc: * $p < 0.05$ versus PEG-Fib, $n = 6$.

279x215mm (300 x 300 DPI)

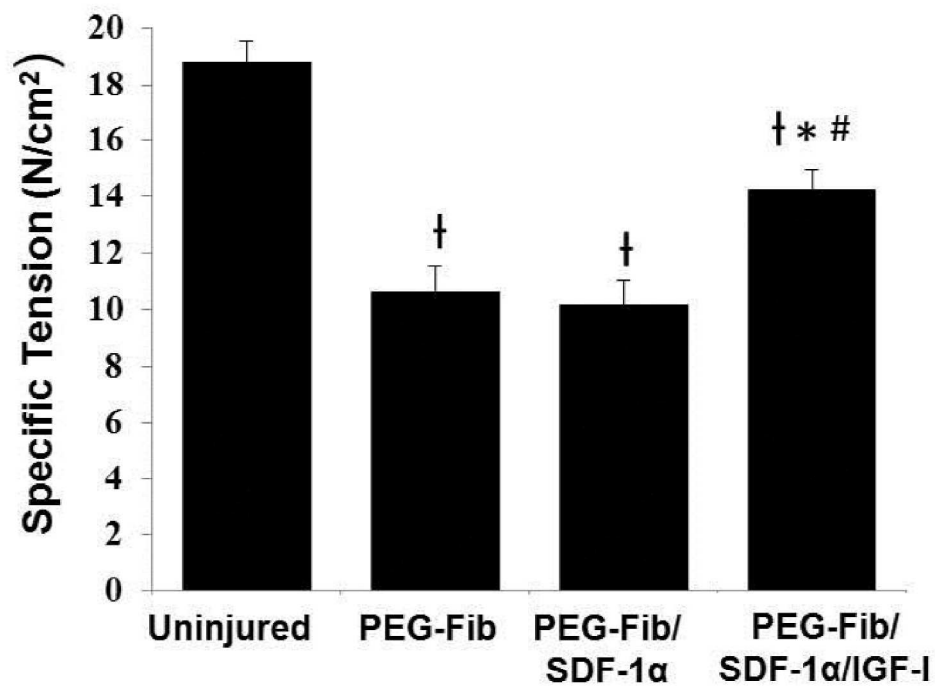


Figure 5. Functional recovery of tetanic tension among treatment groups 14 days after I/R injury. Specific tension (SP0) of the LGAS was measured in situ for the following groups: PEGylated fibrin (PEG-Fib), PEGylated fibrin conjugated to SDF-1 α (PEG-Fib/SDF-1), and PEGylated fibrin conjugated to SDF-1 α and IGF-I (PEG-Fib/SDF-1/IGF-I). Values expressed as mean \pm SEM, one-way ANOVA, Tukey post-hoc: † $p < 0.05$ versus uninjured, * $p < 0.05$ versus PEG-Fib, # $p < 0.05$ versus PEG-Fib/SDF-1, $n = 6$
279x215mm (300 x 300 DPI)

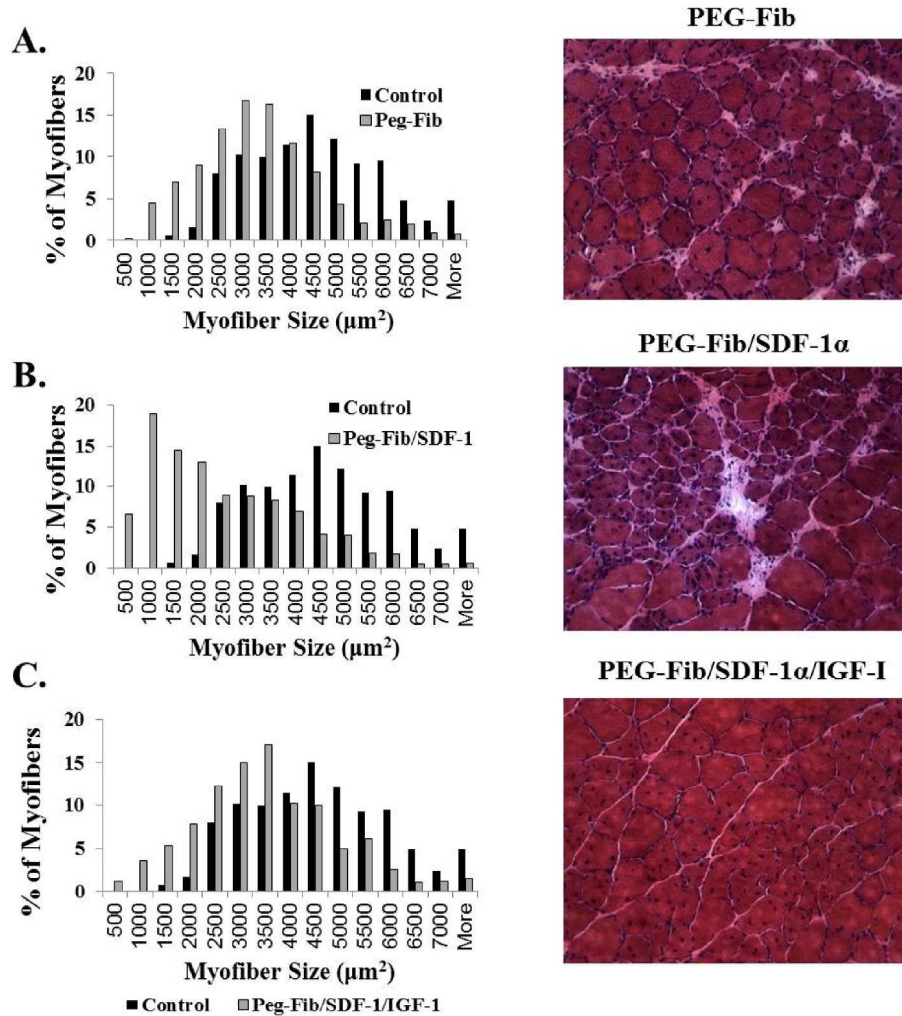


Figure 6. Histological analysis of I/R injured skeletal muscle 14 days post-reperfusion. H&E stained sections were examined for fiber size distribution (200X). Data expressed as percent myofibers of a given area (μm^2). Representative images are included: (A) PEGylated fibrin (PEG-Fib), (B) PEGylated fibrin conjugated to SDF-1 α (PEG-Fib/SDF-1 α), (C) PEGylated fibrin conjugated to SDF-1 α and IGF-I (PEG-Fib/SDF-1 α /IGF-I). 215x279mm (300 x 300 DPI)

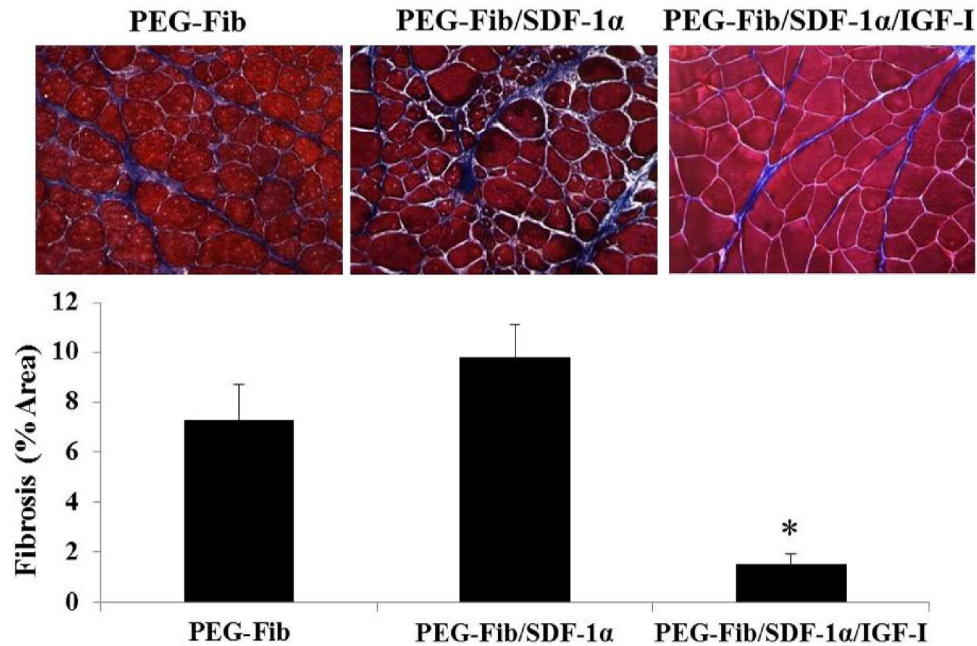


Figure 7. Quantification of collagen deposition in I/R injured skeletal muscle 14 days post-reperfusion. Animals were treated with PEGylated fibrin (PEG-Fib), PEGylated fibrin conjugated to SDF-1 α (PEG-Fib/SDF-1 α), and PEGylated fibrin conjugated to SDF-1 α and IGF-I (PEG-Fib/SDF-1 α /IGF-I) 24h after TK-I/R injury and analyzed 14 days post-reperfusion. Representative images of trichrome staining (200X) where collagen staining is shown in blue (n=3, 3 fields of view/animal). Values expressed as mean \pm SEM, one-way ANOVA, Tukey post-hoc: * p<0.05 versus PEG-Fib group.

279x215mm (300 x 300 DPI)